The Cosmic Ray Measurements Above 1 TeV

Shigeru Yoshida

Institute for Cosmic Ray Research, University of Tokyo
Tokyo 188-8502, Japan

Abstract.

We summarize the updated results on the measurements of cosmic rays with energies above 1 TeV (10^{12} eV). Most of the measurements are consistent with our baseline picture of origins of the cosmic rays that the higher energy extragalactic component is starting to take over the galactic cosmic rays at around $3 \times 10^{18} \sim 10^{19}$ eV. The inconsistency between the measurements on the mass composition at the "Knee" region ($\sim 10^{15}$ eV) needs to be addressed, however, to make more solid conclusion on the origin of the galactic cosmic rays. The hybrid measurement-based approach is shown to be of great help to understand the possible systematics in the different experiments in this energy region. The highlight among the results reported in the conference is the firm detection by the AGASA group of anisotropy of 10^{18} eV cosmic rays associated with direction of the galactic center. In the highest energy end the existence of cosmic rays beyond the expected GZK cutoff (5×10^{19} eV) have been established to challenge our understanding of the high energy particle emissions in extragalactic space.

THE BASELINE PICTURE

The cosmic ray energy spectrum is well represented by a power low form with three bends. The first knee appears around 3×10^{15} eV where the spectral power index changes from -2.7 to -3.0. The second population beyond the knee extends up to $\sim 10^{18}$ eV where the spectral slope further steepen. The third and most energetic population of cosmic rays forms the flatter spectrum above $\sim 3 \times 10^{18}$ eV extending to reach $\sim 10^{20}$ eV region although there is large uncertainty due to poor statistics and resolution.

The most straightforward interpretation of the spectrum features is that the first two populations below 3×10^{18} eV are originated in energetic galactic objects such as supernova remnants. The conventional first order Fermi shock acceleration [1] might be capable of producing these particles at the sites within our galaxy, although many concerns about the effectiveness still remain to be resolved. The most energetic population is likely to be produced by extragalactic objects. The simple

dimensional requirements originally proposed by Hillas [2] rules out most astronomical objects in the universe as shown in Figure 1 because acceleration sites must be considerably large enough for particles to gain sufficient energy before they escape. In addition too strong magnetic field and/or too dense matter and radiation field at the site would result in significant energy loss during their acceleration. Hence only a few objects survives for possible sources and most of them are extragalactic such as the radio galaxies "hot spot" [3].

The picture above has been our baseline concerning the origin of cosmic rays. This "standard model" predicts some measurable features. The "knee" should be formed by confinements efficiency by magnetic field in our galaxy and/or acceleration efficiency of particles as a function of electric charge, both of which leads to transition of the cosmic rays mass composition around the knee from light to heavy dominated primaries. The galactic magnetic field should smear out the directionality of the cosmic rays providing isotropic arrival direction distribution but there might be a chance to see an anisotropy associated in our galactic plane above 10^{18} eV where the galactic magnetic field is not high enough to mix up the trajectories of cosmic ray protons from the galactic sources. If the third and most energetic population is extragalactic in origin, the spectrum should have a real end by the GZK cutoff [4,5] formed by the inelastic collisions of the cosmic ray nucleon primaries on the Cosmic Microwave Background (CMB) [6]. An isotropic extragalactic source distribution will most likely lead to an isotropic arrival distribution in this population. However, as the energy is high enough, the extragalactic magnetic field will be incapable of bending the particle trajectories too much. Consequently there may be some small anisotropy there depending on the (extragalactic) source distribution, strength of the magnetic field, and the mass composition of the highest

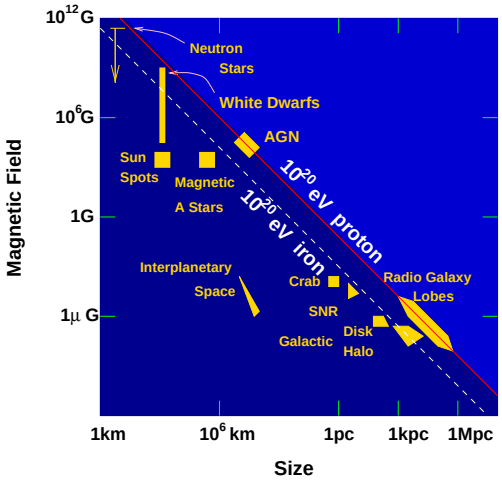

FIGURE 1. The Hillas diagram showing possible sites for acceleration of particles up to 10^{10} eV.

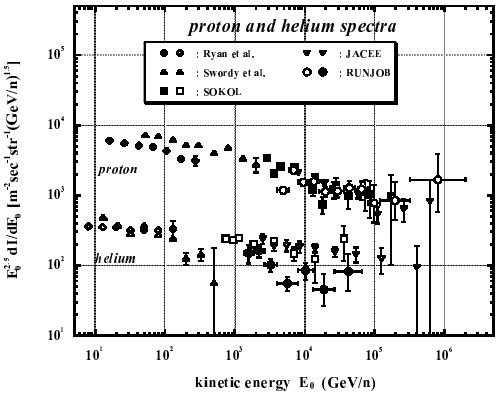

FIGURE 2. The cosmic ray proton and helium energy spectrum below 100 TeV with the updated measurements by the RUNJOB collaboration.

energy cosmic rays.

Now let us check the consistency of these features with the observations reported in the conference.

THE COSMIC RAYS BELOW 100 TEV: DIRECT MEASUREMENTS

In this energy range the updated results were reported from the RUNJOB collaboration presenting their direct measurements of cosmic ray protons, helium and other nuclei [7]. The proton spectrum is almost parallel to that of helium up to $\sim$ 100 TeV as shown in Figure 2. There is no signature of any cutoff of the protons that the JACEE group had reported in the Calgary ICRC and it has now been well established that the all composition including the heavy component constitutes spectra of power low form without bending at least below 10 TeV. No evidence of steepening has emerged. This fact has suggested that no matter how the cosmic ray particles in this energy range are accelerated, same mechanism rules the particle emission and powers cosmic rays up to the knee region. In order to reveal the mechanism, however, it should be strongly encouraged to extend the reliable measurements to the knee region where at least all particle spectrum steepen. One requires detection of any variations from the simple power low spectrum to make real progress on our understanding of the cosmic ray origin. The galactic magnetic field ruins the directionality and timing information of the charged particles and nothing would be truly understood only by observing the unchanged power low spectra.

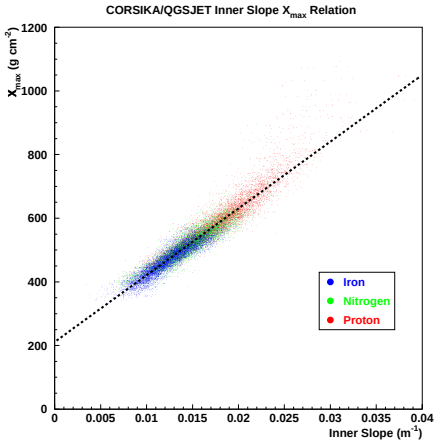

FIGURE 3. The correlation between the inner slope of the lateral distribution of the Cherenkov light pool and X_{max} obtained by Monte Carlo simulation by the BLANCA group.

THE COSMIC RAY COMPOSITION AT THE KNEE

Whether mass composition of cosmic rays is changed at the knee region (100TeV$\sim$ 10^{16} eV) is a key to understand their galactic origin. Several observations have been presented in this conference: The ones with the traditional technique based on the muon contents in extensive air showers and the ones using the Cherenkov radiation from air showers to estimate their longitudinal shower profile. The later observations opened up the new possibility to measure the position of shower maximum in the atmosphere (X_{max}) which is sensitive to the composition of the primary particles. Protons will experience their first interaction deeper in the atmosphere than heavy nuclei of the same energy. Proton showers are also expected to develop slowly than heavy primary showers. Hence the distribution of X_{max} can tell the primary chemical composition. The slope of lateral distribution of the Cherenkov light pool is a good indicator of X_{max} as shown in Figure 3 and the precise measurement of the Cherenkov emission from air showers is one of practical method to study the mass composition.

The CASA-BLANCA group has presented their first results with this method based on the Cherenkov measurement [8]. The BLANCA is an array of 144 Cherenkov detectors covering 0.2 km^2 area of the CASA array that was originally built for VHE γ-ray astronomy. They reconstructed the Cherenkov lateral distribution using the shower geometry determined by the CASA array. As described above, the inner slope of the lateral distribution is used for estimation of X_{max} while the Cherenkov light intensity at 120 m from the shower core (C_{120}) is the primary energy indicator [9]. The results are summarized in Figure 4 indicating the mass composition becomes heavier with the primary energy that would be consistent with our baseline picture of the cosmic ray origin.

Here several remarks must be made on their results. Although the *absolute*

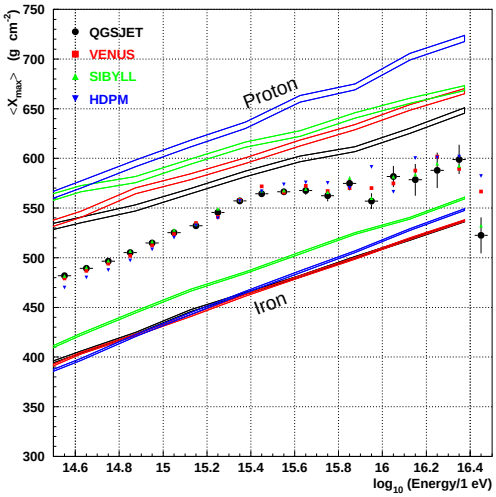

FIGURE 4. The X_{max} as a function of primary energy of cosmic rays measured by the BLANCA detectors. The predictions simulated by several different interaction models are also shown for comparison.

number of X_{max} as a function of primary composition depends strongly on the hadronic interaction models we know little beyond the accelerator energy, the *slope* of X_{max}, *i.e.*, elongation rate dX_{max}/dE is rather robust. Thus the change of the slope they detected at around 3×10^{15} eV is a reliable signature to suggest the mass composition is indeed heavier in the knee region. This bending has occurred in the middle of their energy range in the measurement and the triggering bias or any other experimental systematics would be unlikely to form the bending.

As we expect in the baseline picture, the shift of the mass composition towards

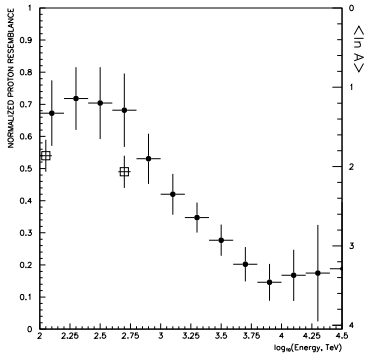

FIGURE 5. Composition trend of CASA-MIA data based on the KNN test.

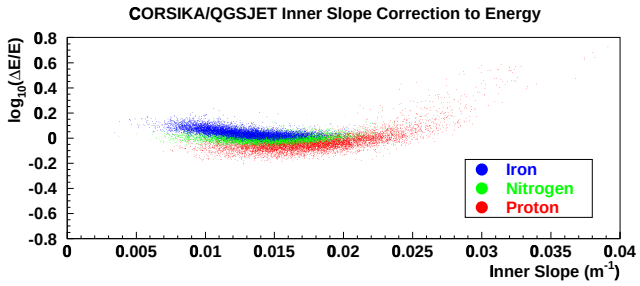

FIGURE 6. Composition bias in the primary energy estimation obtained by Monte Carlo simulation by the BLANCA group. One can see that the correction depends BOTH the inner slope and primary composition.

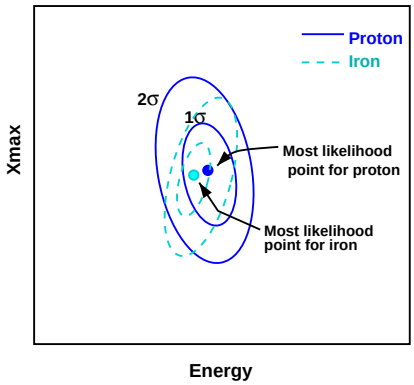

FIGURE 7. A conceptual likelihood contour map showing the correlation between estimated energy and X_{max} for an event observed. The errors of energy and X_{max} estimations are correlated.

heavier primaries has also been detected by the other observations based on the traditional method using the muon density in air showers. The CASA-MIA group measured the muon density as a function of electron size of the shower showing the gradual shift of the composition to heavier primaries [10]. They also performed the advanced study, so called the KNN test, to show the shift. They examined three parameters sensitive to composition: the density of electrons, the slope of the lateral distribution near the core, and the muon density at large core distance. They are tabulated both for data and for simulation events to define the likelihood of "proton-like" and "iron-like" by sampling the neighbors of the simulation data set around each CASA-MIA data in the three parameter space. Figure 5 shows the results of the KNN test applied to their data. The "proton resemblance" is a sort of likelihood probability that the cosmic ray composition in each energy bin is pure proton. The details are described in the reference [10]. One can see there appears to be the same trend of the shift to heavier masses. The well advanced observation made by the KASCADE group who has measured not only muon size but also hadron size distributions has obtained the same tendency [11].

It should be noted, however, that there exists non-negligible discrepancy between

the observations. The DICE group measured the Cherenkov angular distribution to claim that the mass composition seems gradually *lighter* with primary energy [12]. Even among the experiments that favor the shift to heavier masses, the fraction of "light" component at the same energy is quite different each other. The different experimental methods which rely on X_{max}, electron/muon size, and hadron size give different numbers of average mass as seen in the KASCADE experiment. Let us make some remarks here to settle the issues. First we should make an attempt to obtain the measurements relatively insensitive to the hadronic interaction models. This is not only because our knowledge on the hadronic interactions is very limited in this energy range but because we have already seen that any model available now failed fully to describe our observations as the QGSJET model has given primary masses significantly heavier than iron at energies of 10 PeV to the KASCADE hadron size data [11]. The bending of the X_{max} elongation curve detected by the BLANCA shown in Figure 4 can be a good example of experimental results insensitive to the interaction models. The question we should ask then is to how extent this flattening of X_{max} elongation is free from experimental systematics. In fact the primary energy estimation depends on the inner slope, the X_{max} indicator, and one needs to make an appropriate correction in the energy estimation as shown in Figure 6. What can be even worse is that this correction also depends on the primary particle mass. This bias also appears in event by event basis in the estimation of X_{max} and primary energy as conceptually shown in Figure 7. One should rule out the possibility that the bias and the limited experimental resolution

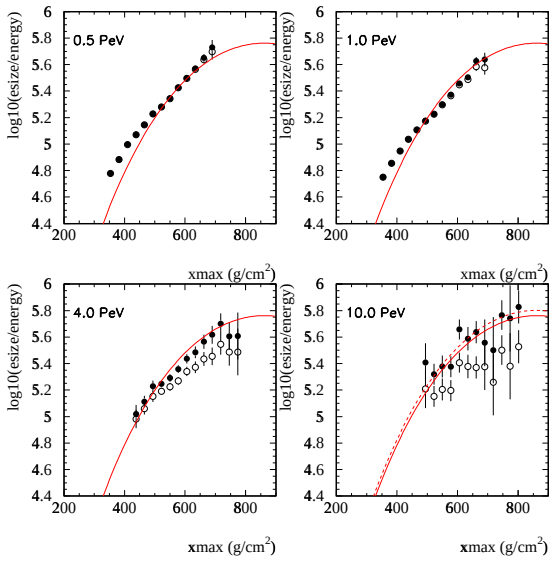

FIGURE 8. The correlation between normalized electron size and X_{max} at different energies. The solid curve shows the expected correlation calculated by the Gaisser-Hillas shower profile function.

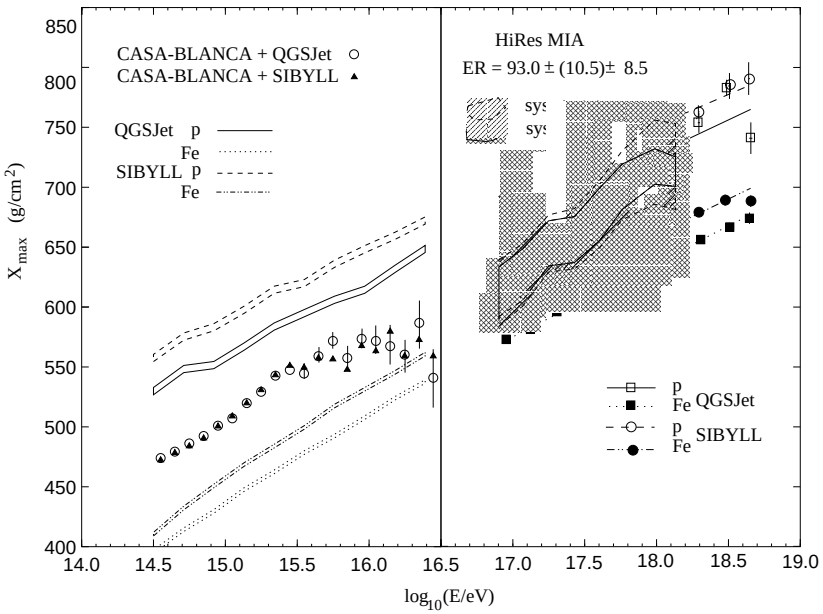

FIGURE 9. X_{max} versus primary energies between 10^{14} and 10^{18} eV.

discussed here could have indeed caused the feature of the bending.

Another way to study the systematics is the *hybrid* measurement. The DICE group has performed the remarkable job along this direction [12]. Figure 8 shows the correlation between normalized electron size measured by the CASA surface array and X_{max} determined by the DICE's Cherenkov light measurement. The electron size at ground level should be a function of the shower energy and X_{max} following the longitudinal shower profile. If they are measured with no bias, we should see the clear fit of the electron size with the energy and X_{max}. The good agreement between the expected function and the data has been obtained at 1 PeV range but a slight discrepancy has been detected in the higher energy range. This illustrates the power of redundant hybrid measurements to explore systematics problems. The BLANCA experiment should be also capable of this kind of hybrid analysis using the CASA/MIA data. Future hybrid analysis by them or the HEGRA experiment [13] can be expected to resolve systematics problems. Wait for the ICRC 2001!

THE MASS COMPOSITION ABOVE THE KNEE

The redundant hybrid detection has also shown its power for measurement of mass composition beyond the Knee region. The players here are the MIA array to measure the muon density of air showers and the HiRes prototype detector to deduce X_{max} by reconstruction of longitudinal shower profile imaged by air fluorescence light emission from air showers [14]. Unified information from both MIA and HiRes gives precise determination of shower geometry which leads to better resolution of energy and X_{max} with less systematics.

Figure 9 shows the average X_{max} as a function of primary cosmic ray energies together with the CASA-BLANCA observation at the Knee region for comparison. One see the gradual shift towards lighter primaries above 10^{17} eV although one cannot rule out a possibility of no shift because of their poor statistics. Measurement in wider span of energies with more statistics is definitely necessary for concrete conclusion, but the results can be interpreted by appearance of extragalactic cosmic ray protons. The stereo measurement by the full operation of the HiRes detector would tell us whether this view is true or not.

PRESENCE OF THE HIGH ENERGY GALACTIC COMPONENT

It is true that the HiRes-MIA hybrid measurement has shown that the observed data at 10^{18} eV is consistent with existence of primary protons, but not all of them is coming from extragalactic space. Some still arrives from our own Galaxy. This is what the AGASA detector has seen at 10^{18} eV: Strong anisotropy associated with the Galactic Center [15]. This is the first clear evidence of existence of galactic component of high energy cosmic rays.

The AGASA detector is the giant air shower array covering 100 km^2 area and started its operation in 1991 [16]. 29207 events in total observed in the range of $10^{18.0} \sim 10^{18.5}$ eV exhibited strong anisotropy in the first harmonic analysis. The Rayleigh k parameter reaches 12.9 for events with energies between 1×10^{18} and 2×10^{18} eV. The chance probability is $e^{-12.9} \simeq 2.5 \times 10^{-6}$.

This strong anisotropy was found to arise from event excess near the galactic

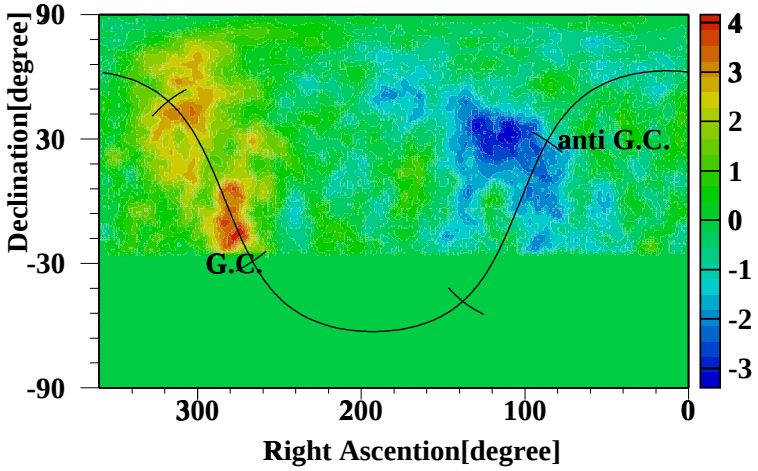

FIGURE 10. Significance map of excess or deficit events. Events within radius of 20° are summed up in each bin.

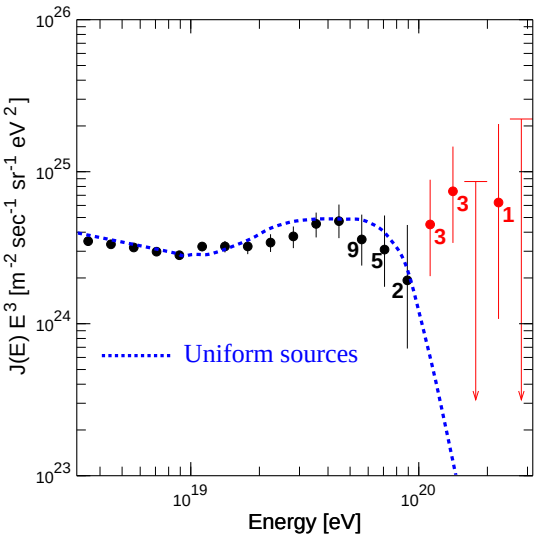

FIGURE 11. The energy spectrum using the data until June 1999 measured by the AGASA.

center and the Cygnus region [17]. Figure 10 shows the arrival direction distribution in equatorial coordinates for events with energies of $10^{18.0} \sim 10^{18.5}$ eV. 4σ and 3σ excess can be seen while there is a deficit in the cosmic ray intensity near the direction of anti-Galactic Center. This result suggests existence of cosmic ray protons originated in our galaxy because heavy primaries would lose their original directionality due to the galactic magnetic field. $\sim$ 30 % of the proton abundance is consistent with this observation [18], while the galactic neutron hypothesis is another possible explanation [17].

THE HIGHEST ENERGY COSMIC RAYS

The observations of cosmic rays at the highest energy end has started to provide some signatures concerning their origin for the last decade: Events with energies will beyond 10^{20} eV [19,20]; lacking for remarkable astronomical objects in their arrival directions [21,22]; no enhancement of the arrival directions associated with the galactic plane; possible event clusters above 4×10^{19} eV arriving from directions well away from the galactic plane [23]. The full accumulation of the data by the AGASA group has further enhanced these features.

It was announced in this conference that the AGASA has now seen seven events above 10^{20} eV [24]. In Figure 11 is shown the updated measurement of the energy spectrum above 3×10^{18} eV. In fact some attentions must be paid regarding the energy resolution of the seven events. Let us give you an example. Figure 12 shows the event with estimated energy of 1.4×10^{20} eV recorded in January of 1996. This event has certain probability of its primary energy being below 10^{20} eV. The χ^2 distribution in the energy estimation procedure is plotted in Figure 13. It is seen that 2σ lower bound is 8×10^{19} eV, surely below 10^{20} eV. However, on the other

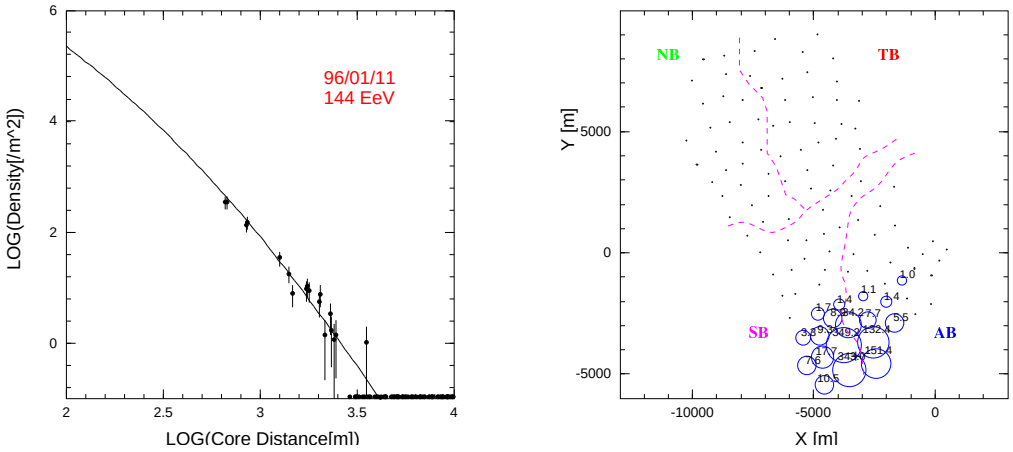

FIGURE 12. The AGASA event with estimated energy of 1.4×10^{20} eV.

hand, this figure illustrates that any trial to reduce the estimated energy causes rapid raising of χ^2 while even higher energies could be reasonable without raising χ^2 too much by having core location of the shower closer to the array boundary. Consequently it is difficult to overestimate the primary energy. As plotted by the dash curve in Figure 11, the GZK mechanism allows detection of SOME events with energies beyond 10^{20} eV due to the limited energy resolution as we discussed here, but not much. For the present AGASA exposure of 3.7×10^{16} m^2 sec sr and their expected energy resolution, one expect ~ 0.6 event above 10^{20} eV which is inconsistent with the detection of the seven events.

The HiRes collaboration has also presented its preliminary measurement of the energy spectrum by a single air fluorescence eye [25]. It detected seven events above 10^{20} eV with similar exposure of the AGASA. The energy resolution and systematics for those events must be studied carefully for solid conclusion, but the result is not inconsistent with the AGASA's observation. The fact that the absolute

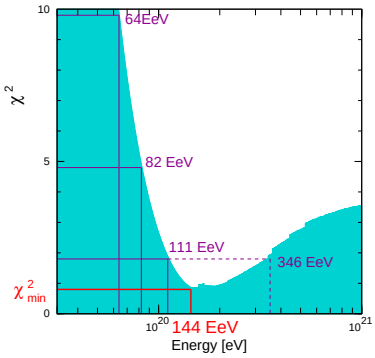

FIGURE 13. The χ^2 distribution on the energy estimation of the event shown above.

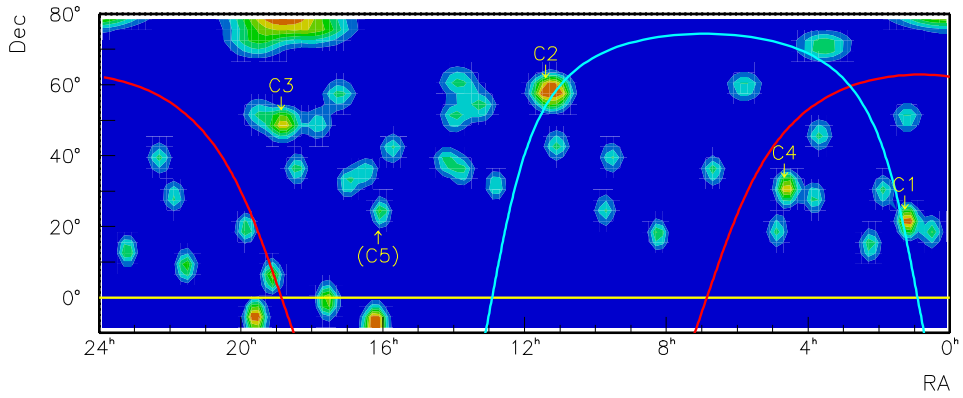

FIGURE 14. Significance map of cosmic ray excess and deficit above 4×10^{19} eV observed by AGASA. The solid curves indicate the Galactic and supergalactic plane.

intensity of the cosmic ray flux measured by a *single* HiRes eye is almost as same as that measured by *stereo* eyes of the old Fly's Eye indicates that the energy resolution of the HiRes has truly been improved significantly compared to the old Fly's Eye. The full data from the stereo HiRes is expected to provide complete evidence of existence of cosmic rays above 10^{20} eV and signatures of their origin.

The arrival directions of the events at the highest energy end are completely isotropic in terms of large-scale anisotropy. The small-scale anisotropy which appeared in form of three pairs of cosmic rays above 4×10^{19} eV in the 1995 AGASA data set [23], however, has now been enhanced in the recent data forming one triplets and three doublets [26]. In Figure 14 is presented the contour map of the cosmic ray excess or deficit with respect to an isotropic distribution above 4×10^{19} eV, the predicted energy above which the cosmic ray flux is attenuated due to the GZK mechanism if the sources are located universally in extragalactic space [27,28]. The doublets, two events within a separation angle of 2.5°, are C1, C3 and C4. One of the members of C1 is the 2×10^{20} event, the most energetic event recorded by AGASA [19]. C2 is the triplet, a cluster of three events. The chance probability of the clustering is 0.32% for doublets and 0.87 % for triplets according to the Monte Carlo simulation.

It is remarkable that none of those clusters is on the Galactic plane suggesting extragalactic objects are responsible for them. Some galaxies were found in their arrival directions: An interacting galaxy Mrk 40 for C2 triplet , Mrk 359 for C1 doublet including the highest energy event. The distance to these galaxies is ~ 70 Mpc, which is too far away for very energetic particles above 10^{20} eV to arrive at earth due to the GZK mechanism, however.

THE GZK CRISIS?

The GZK cutoff has been the centerpiece of the highest energy cosmic ray physics that would provide observable proof of the extragalactic origin. It is now clear that this simple picture needs to be corrected or modified. Several proposal to evade the GZK mechanism or modify the simplest version of the GZK model were discussed in the conference.

- Neutron Stars in our galaxy may have ability to power energies of 10^{20} eV into microscopic particles. Angela Olinto argued that young neutron star wind is indeed capable of acceleration of irons up to $\sim 4 \times 10^{20}$ eV [29]. Photodisintegration at the acceleration sites might give difficulties against acceleration of heavy nuclei, however. The event clusters detected by AGASA cannot be explained by this model, but further accumulation of data as well as measurements of primary composition at highest energy end are necessary to test the model.

- If galaxies in our local neighborhood are the highest energy cosmic ray emitters, the GZK cutoff does not appear because their distances are so close. A spatial distribution of sources that follows the luminous matter distribution in the local universe rather than the isotropic distribution would result in the spectrum consistent with the AGASA observation [30]. Peter Biermann [31] and Glennys Farrar discussed radio galaxy M87 with the possible $\sim \mu$G order magnetic halo might explain the observation. The AGASA's event clusters disfavor this idea but the model is very "economical". Extensive studies will be valuable to check the consistency.

- The cold dark matter trapped in the Galactic halo might be origin of most energetic cosmic rays [32,33]. It predicts anisotropy associated with the Galactic center, but the AGASA data above 10^{19} eV is negative to the model [26]. More statistics is required to investigate anisotropy at 10^{20} eV, which would be a real test for this idea.

- Superhigh energy neutrinos possibly emitted from powerful far-away sources could collide with nearby cosmological neutrinos with a mass of $0.1 \sim 1$ eV generating cosmic rays beyond the GZK cutoff energies [34,35]. The extensive numerical calculation has shown this mechanism would explain the observed energy spectrum without violating the constraints obtained by high energy γ-rays, cosmic rays, and neutrino observations *if* the maximum neutrino energy reaches to $\sim 10^{22}$ eV and the relic neutrino dark matter is clustered on the supercluster scale ($\sim$ 5Mpc) [36]. Primary particles with energies beyond 10^{20} eV have been predicted to be protons and γ-ray photons whose flux intensities are comparable each other [36]. The mechanism to radiate superhigh energy neutrinos is unknown, however.

The above possibilities predict specific observations on anisotropy and mass compositions of the highest energy cosmic rays. Especially it would be of great help to

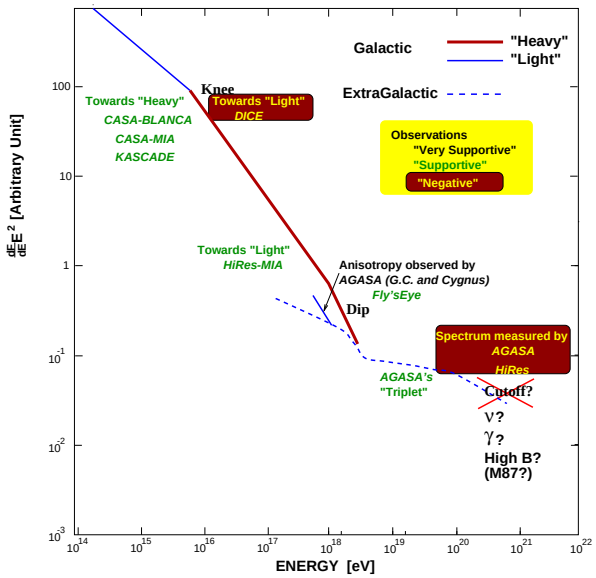

FIGURE 15.

search for γ rays or neutrinos at those energies and/or discover the highest energy cosmic ray point sources because they would not allow the models to adjust their poorly known parameters like strength of the magnetic field or size of the halo for fitting the observations.

SUMMARY

Figure 15 summarizes the observations along with the standard predictions. Our baseline picture of the cosmic ray origin described in the first part of this paper still survives but the new data presented in the conference requires at least its partial revision. We expect data presented at the next ICRC 2001 to reveal *how* to revise it.

ACKNOWLEDGMENTS

The author wishes to thank the conference organizers for their warm hospitality at this conference. He also wishes to acknowledge very valuable discussions and exchanges of the data and interesting ideas with Zhen Cao, Charles Jui, Bruce Dawson, Daniele Fargion, Glennys Farrar, Brian Fick, Lucy Fortson, Joe Fowler, Karl-Heinz Kampert, Jim Matthews, Toru Shibata, Todor Stanev, Simon Swordy, Masahiro Takeda, and Masahiro Teshima. This work is partly supported by the Inamori Foundation.

REFERENCES

1. Drury L. O'C., in *Astrophysical aspects of the most energetic cosmic rays* p.252 (World Scientific, Singapore) (1991)
2. Hillas A. M., *Ann.Rev.Astron.Astrophys.* **22** 425 (1984).
3. Rachen, J. P., and Biremann, P. L., *Astron.& Astrophys*, **272**, 161 (1993).
4. Greisen, K., *Phys. Rev. Lett.* **16**, 748 (1966).
5. Zatsepin, G. T., and Kuzmin. V. A., *Sov.Phys. JEPT Lett.* **4**, 78 (1966).
6. Yoshida. S., and Dai, H., *J. Phys. G: Nucl. Part. Phys.* **24**, 905 (1998).
7. RUNJOB collaboration, *26th ICRC* **3**, 163 (1999).
8. Fortson, L. F., et al., *26th ICRC* **3**, 125 (1999).
9. Fortson, L. F., et al., *26th ICRC* **5**, 332 (1999).
10. Glasmacher, M. A. K., et al., *26th ICRC* **3**, 129 (1999).
11. Kampert, K. -H., et al., *26th ICRC* **3**, 159 (1999).
12. Swordy, S.P., and Kieda, D. B., *26th ICRC* **3**, 144 (1999).
13. Röhring, A., et al., *26th ICRC* **3**, 152 (1999).
14. Abu-Zayyad, T., et al., *26th ICRC* **3**, 260 (1999).
15. Hayashida, N., et al., *26th ICRC* **3**, 256 (1999).
16. Yoshida. S., et al., *Astropart. Phys.* **3** 105, (1995).
17. Hayashida, N., et al., *Astropart. Phys.* **10** 303, (1999).
18. Lee, A. A., and Clay, R. W., *J. Phys. G: Nucl. Part. Phys.* **21**, 1743 (1995).
19. Hayashida, N., et al., *Phys. Rev. Lett.* **74**, 3491 (1994).
20. Bird, D. J., et al., *Astrophys. J.* **441**, 144 (1995).
21. Elbert, J. W., and Sommers, P., *Astrophys. J.* **441**, 151 (1995).
22. Halzen, F., et al., *Astropart. Phys.* **3** 151, (1995).
23. Hayashida, N., et al., *Phys. Rev. Lett.* **77**, 1000 (1996).
24. The AGASA collaboration *26th ICRC* **3**, 252 (1999).
25. Abu-Zayyad, T., et al., *26th ICRC* **3**, 264 (1999).
26. Takeda, M., et al., *26th ICRC* **3**, 276 (1999); *Astrophys. J.* **522**, 225 (1999).
27. Yoshida, S., and Teshima, M., *Prog. Theor. Phys.* **89**, 833 (1993).
28. Protheroe, R.J., and Johnson, P., *Astropart. Phys.* **4**, 253 (1996).
29. Olinto, A. V., *26th ICRC* **4**, 361 (1999); *astro-ph/9911154* (1999).
30. Media Tanco, G. A., *26th ICRC* **4**, 346 (1999).
31. Ahn., E-J., et al., *astro-ph/9911123, submitted to Phys. Rev. Lett.* (1999).
32. Kuzmin, V. A., and Rubakov, V. A., *Phys. Atom. Nucl.* **61**, 1028 (1998).
33. Berezinsky, V., Kachelriess, M., and Vilenkin, A., *Phys. Rev. Lett.* **79**, 4302 (1997).
34. Fargion, D., Mele, B., and Salis, A., *26th ICRC* **4**, 287 (1999); *Astrophys. J.* **517**, 725 (1999).
35. Weiler, T. J., *Astropart. Phys.* **11**, 303 (1999).
36. Yoshida, S., Sigl, G., and Lee, S., *Phys. Rev. Lett.* **81**, 5505 (1998).